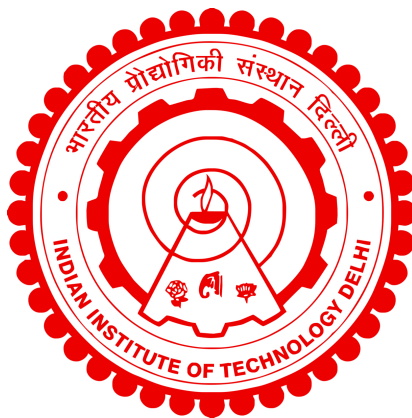


WETTABILITY QUANTIFICATION IN RESERVOIR ROCKS USING TRACERS

DEEPSHIKHA SINGH



DEPARTMENT OF CHEMICAL ENGINEERING

INDIAN INSTITUTE OF TECHNOLOGY DELHI

DECEMBER 2023

© Indian Institute of Technology Delhi (IITD), New Delhi, 2023

**WETTABILITY QUANTIFICATION IN RESERVOIR
ROCKS USING TRACERS**

by

DEEPSHIKHA SINGH

Department of Chemical Engineering

Submitted

in fulfilment of the requirements of the degree of Doctor of Philosophy

to the



INDIAN INSTITUTE OF TECHNOLOGY DELHI

DECEMBER 2023

Dedicated to my family ...

*“Success is the result of perfection, hard work, learning from failure,
loyalty, and persistence”.*

Colin Powell

Certificate

This is to certify that the thesis entitled “**Wettability Quantification in Reservoir Rocks Using Tracers**”, submitted by **Deepshikha Singh** to the Indian Institute of Technology Delhi, for the award of the degree of **Doctor of Philosophy**, is a bonafide record of original research work carried out by her under our supervision in conformity with rules and regulations of the institute.

The results contained in this thesis have not been submitted in part or in full to any other University or Institute for the award of any degree or diploma to the best of our knowledge.



Prof. Jyoti Phirani

Associate Professor

Department of Chemical Engineering

Indian Institute of Technology Delhi.

New Delhi, 110016, India

Prof. Shantanu Roy

Institute Chair Professor

Professor, Department of Chemical

Engineering

Indian Institute of Technology Delhi.

New Delhi, 110016, India

Acknowledgements

I would like to give credit for this work to everyone who has stood by me and constantly inspired me throughout my PhD. Everything that I have achieved is because of their immense support and encouragement. First and foremost, I would like to express my deepest gratitude to my guide and mentor, **Prof. Jyoti Phirani**. Her constant motivation, persistent and patient teachings and expertise have facilitated this work immensely. I am grateful to her for her creative thoughts and the outstanding academic freedom I was offered during this work. I firmly believe that the work ethic, discipline, and focused approach I have learnt from her will keep inspiring me throughout my career.

I am thankful to my co-supervisor, **Prof. S. Roy**, for the invaluable input in this work. His knowledge, resourcefulness and critical reviews have greatly helped me in this work. I am thankful to my research review committee members **Prof. K. K. Pant**, **Prof. Vikram Singh** and **Prof. S. S. Bahga**, for their timely and invaluable inputs in this work. Their knowledge, resourcefulness and critical reviews have greatly helped me in this work. The suggestions from the committee members during the research seminars have helped me to explore and improve my work.

I am very thankful to the Department of Chemical Engineering, Indian Institute of Technology Delhi, for conveniently providing the lab space and facilities to carry on my work. I am also thankful to the Indian Institute of Technology Delhi for providing me with the opportunity to learn, grow and nurture me in all aspects of life. I want to thank my friend, **Mr. Sunil Kumar**, who taught me to work on latex, and for his care and support at all times during my stay at IIT Delhi. I am grateful to my lab mates **Dr. Shabina Asraf**, **Dr. Neelam Choudhary**, **Akshit Agrawal**, **Sombir Pannu** and **Mansi** for supporting me professionally and emotionally at all times during my stay at IIT Delhi.

My heartfelt gratitude to my friends **Anubha**, **Rucha**, **Shalaka**, **Akshata**, **Marvi**, **Ashna**, **Halima**, and **Sufiya** for all the encouragement and support throughout my Ph D. Last but not least, my deepest gratitude to my family for constantly encouraging me and believing in my capabilities. I am thankful to my parents, **Shri Shyam Bali Singh** and **Shrimati Geeta Singh**, for nurturing and supporting me in all my choices. I am indebtedly grateful to **my siblings**. I am thankful to my brother and sister-in-law, **Dr.**

Himanshu Singh and **Mrs. Priyanka Singh**, who have been the backbone of my knowledge, care, love and joy in my life. I am thankful to my father-in-law **Shri Raghubansh Narayan Singh**, and mother-in-law, **Shrimati Sunayana Devi Singh**, for nurturing and supporting me in all my choices. My heartfelt thanks to my brother-in-law and sister-in-law, **Mr. Manish Singh** and **Mrs. Katyayani Singh**. I am very thankful to my dear husband, **Mr. R. P. Singh**, for his care, love, support and understanding in nurturing me in all aspects. He is the one who always supported me in my aims and encouraged me to follow my dreams. At last, I am incredibly thankful to my God lord, **Vishnu**, who is always with me in all situations and made me the kind of person that I am.

Deepshikha Singh

Abstract

Wettability is one of the constitutive properties that define a solid surface preference to contact one liquid over another (for instance, the flow of liquids through the capillaries of a rock). Wettability controls the liquid flow characteristics by controlling the capillary pressure in a porous medium during multiphase flow. Wettability and its alteration are crucial across a wide spectrum of natural and industrial applications. These encompass distinct classes of enhanced oil recovery (EOR) methods, namely chemical EOR and Improved Oil Recovery (IOR), along with groundwater remediation, wicks within loop heat pipes, high-performance lithium-ion batteries, CO_2 sequestration, particle coating, advanced printing techniques, catalyst behaviour within packed bed reactors, the textile industry, paper-based microfluidic devices, and membrane distillation. In oil reservoirs, wettability is a crucial parameter for the sediments, significantly impacting the economics of oil production. Depending on the application, a hydrophobic or hydrophilic surface is preferred for a particular application. Therefore, quantifying a porous medium's wettability is essential.

Wettability characterization in porous media presents unique challenges due to surface heterogeneity, limited visual access to the porous structure, and the computational complexity of large-scale micro-imaging. Recognizing the monotonous relationship between liquid-solid interfacial area and contact angle, measuring and correlating liquid-solid interfacial area with liquid saturation holds the potential for real-time wettability quantification at the Darcy scale. However, the influence of flow conditions, grain size, and saturation path on liquid-solid interfacial area remains unknown. This dissertation introduces a novel method to measure liquid-solid interfacial area during multiphase flow within porous media, with a specific focus on its implications for wettability.

In the initial part of the thesis, we experimentally investigate the two-tracer method to quantify liquid-solid interfacial area in multiphase flow scenarios across a smooth porous medium surface. Our findings consistently show that the liquid-solid contact area increases as saturation levels rise. Notably, when comparing oil and water at the same residual phase saturation, oil exhibits less contact with the glass bead surface, attributed to the water-wet nature of the beads.

In the second part of the thesis, we extend our exploration to three distinct wetting states: water-wet, oil-wet, and mixed-wet, under various saturation and flow conditions. Our

observations revealed intriguing trends. In scenarios where oil is the remaining phase and only water flowed through the porous medium, we noted a consistent increase in solid-water interfacial area with rising water saturation. This phenomenon held true for both water-wet and mixed-wet conditions. However, in the case of an oil-wet porous medium, a remarkable reversal occurred as water saturation increased the water-solid interfacial area diminished. This behaviour is attributed to the dynamic rearrangement of oil and water at higher water flow rates. In the oil-wet scenario, increasing the water flow rate increases the capillary number; consequently, the capillary number introduces instability, leading to finger-like fronts. This instability, in turn, reduces the fraction of oil displaced from the pores. When both oil and water coexisted and flowed through the medium, we observed a consistent trend across all wettability cases: the solid-water interfacial area increased alongside water saturation. Furthermore, this trend was accentuated as water wettability increased, aligning with our expectations.

Further, in the third part of the thesis, the two-tracer method has been explored in a natural porous medium to quantify the liquid-solid contact area during the multiphase flow conditions and consider the different parameters that can affect the measured liquid-solid interfacial area. Flow experiments are performed at different wetting phase saturations and flow conditions, i.e. (a) when the organic phase is at residual saturation and (b) when both the organic and the aqueous phases are moving. When the organic phase is at the residual saturation for a water-wet porous medium, it is observed that increasing the flow rate does not change the residual saturation significantly. However, the measured contact area of the aqueous phase with the porous solid increases with an increase in the water flow rate. This is because of the increased capillary number and the corner flow phenomenon in the porous medium. Further, the effect of various parameters, i.e., grain sizes, gravity, surface morphology and flow process, is considered that can affect the measured liquid-solid interfacial area at different flow conditions and different saturations.

Overall, this analysis reveals the parameters that affect the liquid-solid contact area during two-phase flow in a porous medium. Increasing the flow rate does not increase the flowing phase saturations at a residual oil saturation. However, increasing the liquid flow rate increases the liquid-solid interfacial area during the multiphase flow in a porous medium. The presented work provides a strong option for finding a link between pore-scale wettability and Darcy scale wettability.

सारांश

वेटेबिलिटी एक ठोस सतह की परिभाषा करने वाली संवैधानिक गुणों में से एक गुण है जो एक तरल को दूसरे तरल के साथ संपर्क करने की प्राथमिकता को परिभाषित करता है (उदाहरण के लिए, चट्टान की केशिकाओं के माध्यम से तरल पदार्थ का प्रवाह)। वेटेबिलिटी मल्टीफेज़ प्रवाह के दौरान छिद्रपूर्ण माध्यम में केशिका दबाव को नियंत्रित करके तरल प्रवाह विशेषताओं को नियंत्रित करती है। प्राकृतिक और औद्योगिक अनुप्रयोगों के व्यापक स्पेक्ट्रम में वेटेबिलिटी और इसका परिवर्तन महत्वपूर्ण है। इनमें उन्नत तेल पुनर्प्राप्ति (ईओआर) विधियों की अलग-अलग श्रेणियां शामिल हैं, अर्थात् रासायनिक ईओआर और बेहतर तेल पुनर्प्राप्ति (आईओआर), साथ ही भूजल उपचार, लूप हीट पाइप के भीतर विक्स, उच्च प्रदर्शन लिथियम-आयन बैटरी, CO₂ पृथक्करण, कण कोटिंग, उन्नत मुद्रण तकनीक, पैकड बेड रिएक्टरों के भीतर उत्प्रेरक व्यवहार, कपड़ा उद्योग, कागज-आधारित माइक्रोफ्लुइडिक उपकरण और झिल्ली आसवन। तेल भंडारों में, तलछट के लिए वेटेबिलिटी एक महत्वपूर्ण पैरामीटर है, जो तेल उत्पादन की अर्थव्यवस्था को महत्वपूर्ण रूप से प्रभावित करता है। अनुप्रयोग के आधार पर, किसी विशेष अनुप्रयोग के लिए हाइड्रोफोबिक या हाइड्रोफिलिक सतह को प्राथमिकता दी जाती है। इसलिए, झरझरा माध्यम की अस्थिरता को मापना आवश्यक है।

झरझरा मीडिया में वेटेबिलिटी लक्षण वर्णन सतह की विविधता, झरझरा संरचना तक सीमित दृश्य पहुंच और बड़े पैमाने पर सूक्ष्म-इमेजिंग की कम्प्यूटेशनल जटिलता के कारण अद्वितीय चुनौतियां प्रस्तुत करता है। तरल-ठोस इंटरफेशियल क्षेत्र और संपर्क कोण के बीच नीरस संबंध को पहचानते हुए, तरल-ठोस इंटरफेशियल क्षेत्र को तरल संतृप्ति के साथ मापने और सहसंबंधित करने से डार्सी पैमाने पर वास्तविक समय वेटेबिलिटी मात्रा का ठहराव की संभावना होती है। हालाँकि, तरल-ठोस इंटरफेशियल क्षेत्र पर प्रवाह की स्थिति, अनाज के आकार और संतृप्ति पथ का प्रभाव अज्ञात रहता है। यह शोध प्रबंध झरझरा मीडिया के भीतर मल्टीफेज़ प्रवाह के दौरान तरल-ठोस इंटरफेशियल क्षेत्र को मापने के लिए एक नई विधि प्रस्तुत करता है, इसमें वेटेबिलिटी के परिणामों पर विशेष ध्यान केंद्रित है।

थीसिस के प्रारंभिक भाग में, हम प्रयोगात्मक रूप से एक चिकनी छिद्रपूर्ण माध्यम सतह पर मल्टीफेज़ प्रवाह परिदृश्यों में तरल-ठोस इंटरफेशियल क्षेत्र को मापने के लिए दो-ट्रेसर विधि की जांच करते हैं। हमारे निष्कर्ष लगातार दर्शाते हैं कि जैसे-जैसे संतृप्ति स्तर बढ़ता है, तरल-ठोस संपर्क क्षेत्र बढ़ता है। विशेष रूप से, जब समान अवशिष्ट चरण संतृप्ति पर तेल और पानी की तुलना की जाती है, तो तेल कांच के मनके की सतह के साथ कम संपर्क प्रदर्शित करता है, जिसका कारण मोतियों की पानी-गीली प्रकृति है।

थीसिस के दूसरे भाग में, हम अपनी खोज को विभिन्न संतृप्ति और प्रवाह स्थितियों के तहत तीन अलग-अलग गीलापन स्थितियों तक विस्तारित करते हैं: पानी-गीला, तेल-गीला और मिश्रित-गीला। हमारे अवलोकनों से

दिलचस्प रुझान सामने आए। ऐसे परिदृश्यों में जहां तेल शेष चरण है और छिद्रपूर्ण माध्यम से केवल पानी बहता है, हमने बढ़ती जल संतृप्ति के साथ ठोस-जल इंटरफेसियल क्षेत्र में लगातार वृद्धि देखी है। यह घटना जल-गीली और मिश्रित-गीली दोनों स्थितियों के लिए सही साबित हुई। हालाँकि, तेल-गीले झरझरा माध्यम के मामले में, एक उल्लेखनीय उलटफेर हुआ क्योंकि जल संतृप्ति में वृद्धि हुई और जल-ठोस इंटरफेसियल क्षेत्र कम हो गया। इस व्यवहार को उच्च जल प्रवाह दर पर तेल और पानी की गतिशील पुनर्व्यवस्था के लिए जिम्मेदार ठहराया जाता है। तेल-गीले परिदृश्य में, जल प्रवाह दर बढ़ने से केशिका संख्या बढ़ जाती है; परिणामस्वरूप, केशिका संख्या अस्थिरता का परिचय देती है, जिससे उंगली की तरह के मुख्य उभार बन जाते हैं। यह अस्थिरता, बदले में, छिद्रों से विस्थापित तेल के अंश को कम कर देती है। जब तेल और पानी दोनों सह-अस्तित्व में थे और माध्यम से प्रवाहित हुए, तो हमने सभी वेटेबिलिटी मामलों में एक सुसंगत प्रवृत्ति देखी: जल संतृप्ति के साथ-साथ ठोस-जल इंटरफेसियल क्षेत्र में वृद्धि हुई। इसके अलावा, जैसे-जैसे पानी की घुलनशीलता बढ़ती गई, यह प्रवृत्ति हमारी अपेक्षाओं के अनुरूप बढ़ती गई।

इसके अलावा, थीसिस के तीसरे भाग में, मल्टीफ़ेज़ प्रवाह स्थितियों के दौरान तरल-ठोस संपर्क क्षेत्र को मापने के लिए प्राकृतिक छिद्रपूर्ण माध्यम में दो-ट्रेसर विधि का पता लगाया गया है और विभिन्न मापदंडों पर विचार किया गया है जो मापा तरल ठोस इंटरफेसियल क्षेत्र को प्रभावित कर सकते हैं। प्रवाह प्रयोग अलग-अलग गीला चरण संतृप्ति और प्रवाह स्थितियों पर किए जाते हैं, यानी (ए) जब कार्बनिक चरण अवशिष्ट संतृप्ति पर होता है और (बी) जब कार्बनिक और जलीय दोनों चरण चल रहे होते हैं। जब कार्बनिक चरण जल-गीले झरझरा माध्यम के लिए अवशिष्ट संतृप्ति पर होता है, तो यह देखा जाता है कि प्रवाह दर बढ़ने से अवशिष्ट संतृप्ति में महत्वपूर्ण परिवर्तन नहीं होता है। हालाँकि, झरझरा ठोस के साथ जलीय चरण का मापा संपर्क क्षेत्र जल प्रवाह दर में वृद्धि के साथ बढ़ता है। इसका कारण केशिका संख्या में वृद्धि और छिद्रपूर्ण माध्यम में कोने के प्रवाह की घटना है। इसके अलावा, विभिन्न मापदंडों, यानी, अनाज के आकार, गुरुत्वाकर्षण, सतह आकृति विज्ञान और प्रवाह प्रक्रिया के प्रभाव पर विचार किया जाता है, जो विभिन्न प्रवाह स्थितियों और विभिन्न संतृप्ति पर मापा तरल-ठोस इंटरफेसियल क्षेत्र को प्रभावित कर सकता है।

कुल मिलाकर, यह विश्लेषण उन मापदंडों को प्रकट करता है जो झरझरा माध्यम में दो-चरण प्रवाह के दौरान तरल-ठोस संपर्क क्षेत्र को प्रभावित करते हैं। प्रवाह दर बढ़ाने से अवशिष्ट तेल संतृप्ति पर प्रवाह चरण संतृप्ति में वृद्धि नहीं होती है। हालाँकि, तरल प्रवाह दर बढ़ने से झरझरा माध्यम में मल्टीफ़ेज़ प्रवाह के दौरान तरल-ठोस इंटरफ़ेस क्षेत्र बढ़ जाता है। प्रस्तुत कार्य पोर-स्केल वेटेबिलिटी और डार्सी स्केल वेटेबिलिटी के बीच संबंध खोजने के लिए एक मजबूत विकल्प प्रदान करता है।

Contents

Certificate

Acknowledgements

Abstract

Contents

List of Figures

List of Tables

Abbreviations

Symbols

1	Introduction	1
1.1	Motivation	1
1.2	Research Objectives	3
1.3	Thesis Organisation	4
2	Literature Review	5
2.1	Wettability and its importance	5
2.2	Description of wettability at different length scales	8
2.3	Methods used for wettability quantification for porous media	11
2.4	Tracer tests for porous reservoirs	16
2.4.1	Traditionally used tracer tests	16
2.4.2	Tracer tests to assess wettability	17
3	Methodology	21
3.1	Principle of two-tracer method	21
3.2	Estimation of liquid-solid contact area A_T using the two-tracer method	23
3.2.1	Selection of materials	23

3.2.1.1	Porous substrate	23
3.2.1.2	Organic and aqueous phases	24
3.2.1.3	Tracers for oil phase	24
3.2.1.4	Tracer for aqueous phase	24
3.2.2	Tracer concentrations measurement in solution	25
3.2.3	Single-phase flow experiments for K_a estimation	26
4	Solid-liquid interfacial area measurement for a water-wet system	31
4.1	Methodology	32
4.1.1	Materials	34
4.1.2	Tracer concentration measurements using UV-Vis spectrophotometer	35
4.1.3	Estimation of adsorption coefficient K_a by flow experiments	37
4.1.4	Two-phase flow experiments to estimate the solid-fluid interface area	39
4.2	Results and Discussion	40
4.2.1	Single-phase flow experiments	40
4.2.2	Two-phase flow experiments	42
4.3	Summary	48
5	Impact of different wettability on solid-liquid interfacial area and flow conditions	49
5.1	Materials	50
5.1.1	Preparation of the glass beads	51
5.1.2	Flotation test for qualitative wettability characterization	52
5.1.3	Capillary rise experiments and wettability alteration validation	53
5.2	Flow experiments with single-phase	54
5.2.1	Estimation of K_a using single-phase flow experiment	56
5.2.2	Estimation of K_a for STS	58
5.3	Flow experiments with two phases	60
5.3.1	Estimation of solid-water interfacial area A_w	63
5.3.2	Flow experiment with two flowing phases	66
5.4	Validity of the methodology for geological system	69
5.5	Summary	72
6	Impact of grain size, gravity, surface morphology and flow process on water-solid interfacial area	73
6.1	Methods and Materials	74
6.1.1	Experimental setup	74
6.1.2	Tracer test theory	75
6.1.3	Methodology to estimate K_a of the adsorbing tracer	76
6.1.4	Materials	77
6.2	Results	78
6.2.1	Effect of grain size on measured water-solid contact area	78
6.2.1.1	Preparation of the porous medium for multiphase flow	78

6.2.1.2	Estimation of water-solid contact area at residual oil saturation	79
6.2.1.3	Estimation of water-solid contact area with two flowing phases	82
6.2.2	Effect of gravity on measured water-solid contact area	84
6.2.2.1	Estimation of water-solid contact area with residual oil saturation	85
6.2.2.2	Estimation of water-solid contact area with two flowing phases	87
6.2.3	Discussion for 2 mm glass beads experiments	89
6.2.4	Effect of the surface morphology on measured water-solid contact area	92
6.2.4.1	Estimation of water-sand contact area in the sand pack at residual oil saturation	93
6.2.4.2	Estimation of water-sand contact area in the sand pack with two flowing phases	95
6.2.5	Effect of the flow process on measured water-solid contact area in the sand pack	96
6.2.5.1	Estimation of water-solid contact area with residual oil saturation in WF and OF	97
6.2.5.2	Estimation of water-solid contact area when water and oil flow together in WF and OF experiments	99
6.2.5.3	Discussion for sand experiments	100
6.2.6	Validation of the measured water-solid contact area in the natural porous medium	103
6.3	Discussion on wettability and liquid-solid contact area	104
6.4	Summary	105
7	Conclusions and future directions	107
7.1	Future Scope	109
	Bibliography	111
	List of Publications	135
	Bio-data of author	139

List of Figures

1.1	Behaviour of the wetting versus non-wetting liquid/surface	1
2.1	Surface interactions between three phases (solid-water-oil), Here, θ is the angle measured through the water phase, where a water-oil interface meets on the solid surface, σ_{ws} is the interfacial tension between the solid and water phase, σ_{os} is the interfacial tension between the solid and oil phase, and σ_{ow} is the interfacial tension between the water and oil phase.	5
2.2	Types of grains inside the reservoir	6
2.3	Length scale dependent wettability definition in rock-containing systems . .	9
2.4	Contact-angle of the different wetting states of the solid surface	11
3.1	Visualization of pulse input ideal and adsorbing tracer injection, along with their corresponding response curves.	22
3.2	UV-Vis spectrum of the water-tracer.	26
3.3	Schematic diagram of the step-input tracer test flow experimental setup. . .	28
3.4	Workflow for measuring liquid-solid interfacial area in a porous medium during multiphase flow using the proposed two-tracer method. In this figure, τ (min) represents the mean residence time calculated from the cumulative exit age density function $F(t)$. τ_i (min) and τ_a (min) denote the mean residence times of the ideal and adsorbing tracers, respectively. Q (ml/min) is the flow rate of the liquid containing the tracer (m^3/s), and K_a (ml/g) is the adsorption partition coefficient on the solid matrix. A_T (g) represents the total surface area of the porous medium in contact with a liquid during single-phase flow experiments, while A_w (g) is the total surface area of the porous medium in contact with water during two-phase flow experiments. This study assumes a constant surface area per unit weight of the porous medium and utilizes A_T and A_w in mass units (g).	30
4.1	Schematic diagram of the two-tracer method for the pulse and step-input with their corresponding response curve of adsorbing and ideal tracer. . . .	33
4.2	UV-Vis spectrum, together with the Absorbance vs. Concentration curves (three experiments) in the insets for the selected oil and water phase tracer at various concentrations ranging from 10-100 μM (a) IDB-DD solution (b) Red-oil-DD solution (c) FSS-DIW solution (d) STS-DIW solution.	36
4.3	UV-Vis spectrum of the (a) water tracer experiments, and (b) oil tracer experiments.	37

4.4	Formulated $F(t)$ curve at various flow rates from the single-phase flow experiment (three experiments) of the (a) oil tracers, and (b) water tracers.	41
4.5	Comparison of the experimentally calculated MRTs (three experiments) with the theoretically calculated MRTs of (a) oil tracers, and (b) water tracers.	41
4.6	Two-phase flow experiment, when (a) water is a mobile phase, or ‘phase 2’, water tracer (FSS) is being injected (b) oil is a mobile phase, or ‘phase 2’, dodecane tracer (Red-oil) is being injected.	43
4.7	$F(t)$ curves at various flow rates for (three experiments) (a) Dodecane tracers when DD is the mobile phase (b) water tracer when DIW is the mobile phase.	44
4.8	(a) Relationship between the fraction of the glass beads surface area in contact with water (A_w/A_T) and the water saturation (S_w). (b) the fraction of the wetted surface area of the glass beads by the residual phase vs residual phase saturation.	47
5.1	Schematic diagram of the step-input tracer flow experimental setup.	50
5.2	Images of the flotation test at times (a) $t = 0$, (b) $t = 1$ hour, and (c) $t = 24$ hours.	53
5.3	Left: experimental set-up for a capillary rise experiment. Right: the maximum water rises through the various wetting states of glass bead packing after 24 hours.	54
5.4	UV—visible spectrum of the tracer, in the aqueous-phase and after the mixing with the organic-phase.	56
5.5	The tracer breakthrough curves from the single-phase flow experiment at various flow rates and wetting conditions (a) water-wet, (b) oil-wet, and (c) mixed-wet.	59
5.6	Comparison of theoretical MRT with the experimental MRT by the tracer breakthrough curves from the single-phase flow experiment at various flow rates and wetting conditions (a) water-wet,(b) oil-wet, and (c) mixed-wet.	60
5.7	(a) Collected samples of the steady exit streams at a constant time interval left to the right tube (Red liquid is oil and green liquid is water) (b) The total volume of the oil displaced from the water during secondary imbibition from different wetting conditions (c) Profile of the ultimate oil recovery rate by secondary water imbibition mechanism at 0.25 ml/min from the various wetting conditions of the glass beads packing.	61
5.8	Tracer breakthrough curve during two-phase flow experiments, when oil is the remaining phase in the experiments and does not flow at various flow rates and wetting conditions (a) water-wet, (b) oil-wet, and (c) mixed-wet.	64
5.9	(a) Flow rate versus remaining oil saturation in the different wetting condition porous medium and (b) Relationship between the fraction of the glass beads surface area in contact with water (A_w/A_T) and the water saturation (S_w), when oil is the remaining-phase.	65

5.10	Wetting behaviour of glass beads in contact with water. Yellow denotes the solid phase (glass beads), while green signifies the liquid phase (water-tracer solution). The figure illustrates the differential wetting behaviours of water-wet, oil-wet, and mixed-wet glass beads when exposed to water. . . .	66
5.11	Tracer breakthrough curve when both oil and water are simultaneously flowing through the glass beads packing at various flow rates and wetting conditions (a) water-wet, (b) oil-wet, and (c) mixed-wet.	68
5.12	Relationship between the water flow rate with (a) water-saturation, when oil and water simultaneously flow through the porous medium. (b) The behaviour of the quantified solid-liquid interfacial area at various saturations through different wetting conditions in a porous medium.	69
5.13	Comparison of theoretical MRT with the experimental MRT of the tracer break-through curves from the single-phase flow experiment at various flow rates in a sand pack.	70
5.14	Two-phase flow experiment, when oil is the remaining phase in the experiments and does not flow at various flow rates and only water is the mobile phase in the sand pack.	71
6.1	Schematic of flow experimental setup	75
6.2	The effect of grain size on (a) water saturation, (b) the fractional water-solid contact area; at different water injection rates, and (c) the fractional water-solid contact area as a function of the water saturation at different water injection rates, when water is in the mobile phase, and oil is in the residual phase.	82
6.3	Two-phase flow experimental setup. Right side images are the collected samples at different fractions of water and oil flow rates, Green is water, and Red is oil.	83
6.4	The effect of grain size on (a) water saturation, (b) the fractional water-solid contact area; at different water injection rates, and (c) the fractional water-solid contact area as a function of the water saturation at different water injection rates, when water and oil flow simultaneously into the porous medium.	84
6.5	Comparison of the HTE and VTE experimental results to analyse the relationship between (a) water saturation with the water injection rate (b) fraction of the glass beads surface area in contact with water (A_w/A_T) with the water injection rate, and (c) water-solid contact area vs saturation, when water is in the mobile phase, and oil is in the residual phase in the water-wet 2 mm sized glass bead packed system.	87
6.6	Comparison of the HTE and VTE experimental results to analyse the relationship between (a) water saturation with the water injection rate (b) fraction of the glass beads surface area in contact with water (A_w/A_T) with the water injection rate, and (c) water-solid contact area vs saturation when oil and water both flowing simultaneously in the water-wet 2 mm sized glass bead packing.	89

6.7	Comparison of the flow experimental results when the only water flow in the glass beads packing at different oil saturation to analyse the relationship between the water injection rate with (a) water saturations S_w and (b) fractional solid-water interfacial area (A_w/A_T) and (c) A_w/A_T vs S_w	90
6.8	Comparison of the two-phase flow experimental results when oil and water flow together in the glass beads packing to analyse the relationship between the water injection rate with (a) water saturation (S_w) (b) fraction of the glass bead surface area in contact with water (A_w/A_T) and (c) A_w/A_T vs S_w	91
6.9	The scanning electron microscope (SEM) and the X-Ray Diffraction (XRD) analyses at 10-50 degree diffraction; Left glass beads and Right sand.	92
6.10	Comparison of the two-phase flow experimental result performed in the sand pack with the same sized glass bead to analyse the relationship between the water injection rate with (a) water saturation (b) fraction of the sand surface area in contact with water (A_w/A_T), and (c) A_w/A_T vs S_w when water is mobile-phase, and oil is in residual-phase in the packings.	95
6.11	Comparison of the two-phase flow experimental result performed in the sand pack with the same sized glass bead to analyse the relationship between the water injection rate with (a) water saturation (b) fraction of the sand surface area in contact with water (A_w/A_T), and (c) A_w/A_T vs S_w when oil and water flow simultaneously in the packings.	96
6.12	Comparison of the two-phase flow experimental result performed in WF and OF to analyse the relationship between the water injection rate with (a) water saturation (b) fraction of the sand surface area in contact with water (A_w/A_T), and (c) A_w/A_T vs S_w when oil is in the residual-phase and water is only mobile in the sand pack.	99
6.13	Comparison of the two-phase flow experimental result performed in WF and OF to analyse the relationship between the water injection rate with (a) water saturation (b) fraction of the sand surface area in contact with water (A_w/A_T) and (c) A_w/A_T vs S_w when oil and water flow together in the sand pack.	100
6.14	Comparison of the two-phase flow experimental results when water flows at different flow rates in the porous medium at different residual oil saturations to analyse the relationship between the water injection rate with (a) water saturation (S_w) (b) fraction of the solid surface area in contact with water (A_w/A_T) and (c) A_w/A_T vs S_w when oil is the residual phase and water flow in the porous medium.	101
6.15	Comparison of the two-phase flow experimental results when oil and water flow together in the porous medium to analyse the relationship between the water injection rate with (a) water saturation (S_w) (b) fraction of the solid surface area in contact with water (A_w/A_T) and (c) A_w/A_T vs S_w when oil and water flow together in the porous medium.	102

6.16 (a) Behaviour of the wetting versus non-wetting liquid/solid surface. Here we show the surface interactions between three phases (solid-water-oil) when the same volume of liquid is in contact with wetting and non-wetting surface. Here, θ is the angle measured through the water phase, where a water-oil interface meets on the solid surface, σ_{ws} is the interfacial tension between the solid and water phase, σ_{os} is the interfacial tension between the solid and oil phase, and σ_{ow} is the interfacial tension between the water and oil phase, (b) behaviour of the solid-liquid contact area with the contact angle for a given volume of the drop. 105

List of Tables

4.1	Estimated K_a for oil tracer when $V = 61.33$ (ml) ($L = 12.5$ (cm) and $d = 2.5$ (cm)).	42
4.2	Estimated K_a for water tracer when $V = 60.84$ (ml) ($L = 12.4$ (cm) and $d = 2.5$ (cm)).	42
4.3	Experimentally obtained water saturation (S_w) when water is the mobile phase with the saturation calculated by the mass balance.	45
4.4	Experimentally obtained oil saturation (S_o) when oil is the mobile phase, and the saturation calculated by the mass balance.	45
4.5	The calculated surface area of the glass beads in contact with water (A_w), when dodecane is in the residual phase at different flow rates, $K_a = 0.03$ (ml/g).	47
4.6	The calculated surface area of the glass beads in contact with oil (A_o), when water is in the residual phase at different flow rates, and $K_a = 0.05$ (ml/g).	47
5.1	List of chemicals and their properties.	51
5.2	Estimated K_a from the single-phase flow experiments ($V = 47.10$ ml).	59
5.3	The estimated interfacial area of the glass beads in contact with water (A_w), when oil (DD) is the remaining-phase at different flow rates and different wetting conditions ($V = 47.10$ ml , $K_a = 0.027$, ml/g).	64
5.4	Estimation of the fraction of solid-water interfacial area (A_w/A_T) when oil and water are simultaneously flowing through the porous medium at different wetting conditions ($V = 47.10$ (ml), $K_a = 0.027$, (ml/g)).	69
5.5	Estimated K_a from the single-phase flow experiments ($V = 47.10$ ml).	71
6.1	Estimated K_a for the adsorbing tracer ($V = 47.10$ ml).	79
6.2	The estimated water-solid contact area of the cleaned glass beads (A_w) at various residual oil saturation at different flow rates and different bead sizes ($V = 47.10$ ml , $K_a = 0.03$ ml/g).	80
6.3	Estimated K_a from the single-phase flow experiments ($V = 47.10$ ml).	86
6.4	The estimated water-solid contact area (A_w) of the cleaned 2 mm glass beads at various residual oil saturation and different flow rates in different packing orientations ($V = 47.10$ ml).	86
6.5	Estimated K_a for the adsorbing tracer ($V = 47.10$ ml).	93
6.6	The estimated water-solid contact area in the sand pack (A_w) at various residual oil saturation at different flow rates ($V = 47.10$ ml).	94

List of Tables

6.7 Estimated K_a from the single-phase flow experiments in WF and OF ($V = 47.10 \text{ ml}$). 97

6.8 The estimated water-solid contact area (A_w) in the sand pack at various residual oil saturation and different flow rates ($V = 47.10 \text{ ml}$). 98

6.9 Estimation of the fraction of solid-water interfacial area when oil and water are simultaneously flowing through the porous medium at different flow processes ($V = 47.10 \text{ ml}$). 103

Abbreviations

EOR	Enhanced Oil Recovery
IDB	Iodobenzene
FSS	Fluorescein Sodium Salt
STS	Sodium Thiosulfate
DD	Dodecane
DIW	Deionized water
UV	Ultraviolet
MRT	Mean Residence Time
$E(t)$	Exit age density function
$F(t)$	Cumulative exit age density function
RTD	Residence time distribution
TCMS	Trichloro(methyl)silane
PV	Pore Volume

Symbols

A_b	Absorbance (<i>dimensionless</i>)
A_T	Total solid surface area contacted by the liquid (<i>kg</i>)
c	Concentration of solution (mol/m^3)
C_{exit}	Effluent tracer concentration (mol/m^3)
C_T	Injected tracer concentration (mol/m^3)
ϵ	Molar absorptivity ($m^3/(mol.m)$)
$F(t)$	Cumulative exit age density function (<i>dimensionless</i>)
K_a	Adsorption partition coefficient (m^3/kg)
l	Optical path length or cuvette length (<i>m</i>)
ϕ	Porosity (<i>dimensionless</i>)
Q	Flow rate of the liquid containing the tracer (m^3/s)
q_w	Flow rate of water (m^3/s)
q_o	Flow rate of oil (m^3/s)
ρ_L	Density of the liquid (kg/m^3)
τ_i	Mean residence time of the ideal tracer (<i>s</i>)
τ_a	Mean residence time of the adsorbing tracer (<i>s</i>)
A_w	The glass beads surface area in contact with water (<i>kg</i>)
A_o	The glass beads surface area in contact with oil (<i>kg</i>)
V	Bulk volume of the porous substrate (m^3)
S_o	Saturation of oil (<i>dimensionless</i>)
S_w	Saturation of water (<i>dimensionless</i>)
R	Retardation factor (<i>dimensionless</i>)